

Micromachined biomimetic artificial haircell sensors

Chang Liu

Micro and Nano Technology Laboratory, University of Illinois, Urbana, IL 61810, USA

Received 11 May 2007

Accepted for publication 13 June 2007

Published 16 October 2007

Online at stacks.iop.org/BB/2/S162

Abstract

The biological haircell is a modular building block of a rich variety of biological sensors. Using micro- and nanofabrication technology, an engineering equivalent artificial haircell sensor can be developed, imitating the structure and transfer function of the biological haircell. The artificial haircells can be made of hybrid semiconductor, metal and polymers. This paper discusses a number of strategies, using representative material systems, for building artificial haircell sensors and briefly outlines their fabrication method and performance. The motivation for imitating the biological haircell is also discussed to provide a background for this work.

(Some figures in this article are in colour only in the electronic version)

Background

Animals are endowed with superior sensory intelligence. Sensors found in animals are sensitive, have a wide dynamic range, can function in a noisy environment and are often mechanically robust. The biological intelligence entails both sophisticated sensors and signal processing neurons, allowing animals to survive in an unstructured environment.

We are interested in the haircell sensors, a special class of mechanical sensors found in a variety of animal systems. Haircell sensors found in a wide variety of animal species are responsive to flow, vibration, touch, acoustic vibration and gravitational force. There are two general categories of haircell sensors. The biological haircell is a mechanoreceptive neuron with a cilium grown as a part of the neuronal membrane. Mechanical displacement of the cilium will cause the neuron member to undergo mechanical strain, which induces neuron pulse firing. A second class of haircell, often called 'hairlike receptors' in the biological literature, consists of an external auxiliary hair (seta) connected to a neuron membrane. The hairlike receptors may have different mechanical and molecular principles compared with the true neuronal haircells.

In our research, both the haircell neuronal sensors and the hairlike sensors are called haircell sensors as they share a common mechanical transfer function: they turn force/displacement signals into electronic pulses. However, it should be noted that the two different types of sensors work quite differently; hairlike sensors may have a different range

of dimensions than haircells, and may be composed of quite different materials.

Haircell sensors transfer mechanical stimuli into neuronal signals. They are widely used in the biological world, accomplishing a variety of functions in a large number/variety of animals. The functions of haircell sensors include acoustic sensing, balance (gravitational) sensing, vibration sensing, flow sensing and joint angle sensing (for insects). They can be found in a number of species, performing sometimes more than one function in a given animal. For example, some of their functions are as follows.

- (1) Vertebrates (including humans) use haircells in special structures (cochlea) to sense acoustic vibration [1, 2]. The acoustic vibration impinges on our eardrums and induces traveling pressure waves in the cochlea canal. The traveling waves cause the canal membrane to move slightly. Cochlea membranes are directly attached to the free end of haircell cilia. The displacement of the membrane is translated into cilia motion.
- (2) Vertebrates (including humans) also use haircells in our inner ears for balance and equilibrium sensing [1]. In this case, haircells in the inner ear are connected to tiny pieces of mineral deposits that increase the mass at the end of the haircell. A slight tilt of the head, for example, generates an inertial force acting on the haircell due to density differences between the fluid surrounding the cilia and the mass coupled to the haircell tip.
- (3) Insects such as cockroaches and crickets use haircells for flow sensing [3]. In this case, flow moving past the haircell

- imparts a force based on both friction and pressure drag. The drag force sets up a small displacement of the haircell.
- (4) Insects also use haircells for vibration sensing. In the cerci organs of cockroaches and crickets, the haircell cilia develop into a drum-like shape, increasing the mass at the end of each hair. Ground vibration, for example, would be translated into inertial forces acting on the haircell [4].
 - (5) Spiders use haircells on their body to detect flow movement [5]. Such spider sensors can detect displacement energy smaller than the quanta of light, which corresponds to only 4–7 Å of tip displacement [6].
 - (6) Fish uses haircell sensors for flow sensing [7]. The lateral line system, widely found in animals and amphibians, consists of an array of flow sensors made of haircell sensors. Water flow and high frequency hydrodynamic events are imaged by the lateral line through a soft touch sense. The lateral line is capable of sensing water movement caused by predators, prey, continuous flowing water and water disturbances caused by obstacles. The lateral line allows fish to stabilize themselves in turbulent water, to avoid obstacles, to save energy during swimming [8] and to identify predators/prey in water [9].
 - (7) Arthropods (e.g. insects and crustaceans) also use an array of haircells to detect joint movements [1], since animals with external skeletons cannot detect the relative angle of their own body parts with sensors embedded in skin and muscles. An array of haircells is strategically positioned near the joint, such that one part of the appendage touches the array of hairs as it bends. The number of bent hairs corresponds to the degree of hair bending.
 - (8) Haircells have a variety of other applications [10, 11]. For example, hairs are believed to be a part of the bat wing for hydrodynamic imaging and flight maneuvering.

In fact, almost every vertebrate cell has a specialized cell surface projection called a primary cilium [12]. The haircells are also capable of more than sensing functions. For example, active haircells in cochlea change its stiffness to modify its dynamic range, thereby allowing human beings to hear well in noisy acoustic environment [13].

The haircells found in organisms have very small dimensions associated with them. The typical haircell length is on the order of tens of micrometres to 1 mm for flow sensing hairs. Haircells in cochlea are generally smaller than flow sensing structures. Using conventional machining techniques, it is prohibitive to make hairs with integrated signal transduction elements and electronics circuitry with matching dimensions. Advances in micro- and nanoengineering are now sufficient to build sensors that match the dimensions of biological sensors. Being small means the haircells have a correct mechanical interaction with the environment (e.g., flow–structure interaction for flow sensing haircells), minimal intrusiveness to the environment being sensed and ability to fully integrate with integrated microelectronics circuitry for on-site signal processing.

There are several incentives for building man-made artificial haircells [14]. First, the development of man-made haircells will provide a validation platform for studying the biological haircells themselves. The study of the mechanical

behavior of a biological haircell is typically hampered by the lack of equipment and instrument to study live tissues at small scales. By building man-made equivalent systems, it becomes possible to simplify the task of biological studies; instead of studying live cells, one can study a biological mimic.

Secondly, the building of artificial haircells will increase the interest of studying biology, as the task of bioinspired engineering will demand answers to some unanswered questions in biology. This will push the frontier of biological studies.

Thirdly, the artificial haircell will increase the engineering ability of sensor building and potentially reduce the cost of sensors. Integrated sensors are used widely today, from accelerometers in an automotive airbag deployment system to pressure sensors in patient-monitoring devices. Unfortunately, such sensors are generally developed with a large cost (tens to hundreds of millions of dollars) and long time (several years). The reason for this large cost lies in the fact that every sensor has to use unique structure designs, principles and packaging. The cost of developing a sensor includes that of designing, prototyping, fabrication, calibration and validation.

Biological haircells, on the other hand, provide rich functional variation as noted above. The artificial haircell sensor can serve as a modular building block for advanced sensors of various kinds, such as flow sensors, vibration sensors, pressure sensors and touch sensors. They can even be used to perform chemical sensing functions [15]. It is possible to reduce tremendously the cost of designing, calibration and validation by using the modular building block concept.

The success of the integrated circuit industry attests to the power of using modular building blocks for making small-scale devices [16]. Circuits, from simple flash drive memory chips to million-transistor CPUs, are made by putting transistors, an electronics building block, together into larger systems. The transistor is used in all circuit functions, including logic gates, amplifiers, RF receivers and memory, to name a few. As a result, the world is enjoying high-performance integrated circuitry with a relatively low cost.

Overview of artificial haircells

Various types of flow sensors [17], acoustic sensors, pressure sensors [18, 19] and vibration sensors [20, 21] have been developed using both conventional machining and micromachining technologies. They are based on a variety of materials (including semiconductor, oxide and polymers) and principles (including electrostatic sensing, piezoresistive sensing, thermal sensing, etc). A review of the principles of microfabrication technology and microdevices can be found in [14, 22].

However, artificial haircells represent unique challenges to microengineering design and fabrication. The high aspect ratio, vertical, hair must be fabricated using processing steps that are amenable to engineering manufacturing and eventually scaled production. The overall process must be scalable to large areas as the haircells are often used in an array. Ideally, the haircells should be integrated with highly sensitive transduction mechanisms to couple mechanical input

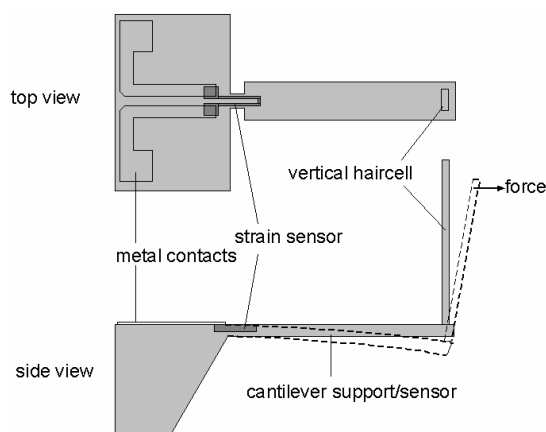


Figure 1. Schematic diagram of a single artificial haircell sensor consisting of a horizontal cantilever with a vertical cilium attached at the free end. The bending of the vertical cilium is sensed using the strain sensor located at the base of the horizontal cantilever.

to electrical output. Further, it is desirable that the haircells be made on a substrate that also houses the integrated electronics elements for signal conditioning and amplification.

My group has developed an artificial haircell sensor by using polymer materials (including polyimide [23, 24], polyurethane [25]) and silicon [26]). Other groups have made haircell sensors. A group at the Twente University developed haircells for flow and acoustic sensing [27]. The hairs are made by using photolithographically patterned SU8 epoxy. Ozaki's group in Japan has developed various types of flow sensors by attaching bonding wires to microstrain gauges [28].

Silicon-based artificial haircells

The schematic diagram of a silicon-based artificial lateral line sensor is shown in figure 1. Each sensor consists of an in-plane cantilever with a vertical artificial cilium attached at the distal, free end. External flow parallel to the sensor substrate imparts friction drag and pressure drag upon the vertical cilium. Due to a rigid connection between the

in-plane cantilever and the vertical cilium, a mechanical bending moment is transferred to the horizontal cantilever beam, inducing longitudinal strain at the base of the cantilever beam. The magnitude of the induced strain can be sensed by many means, for example by using integrated piezoresistive sensors, which change resistance upon deformation. One can interrogate the resistance change by passing a known current through the piezoresistor and monitoring the voltage drop. The piezoresistor can be made by selectively doping regions of the silicon semiconductor substrate. It should be noted that though neurons are used in biology for both sensing and signal conditioning, an engineering equivalent of the neuron is not available, so that signal processing downstream of the sensor is the primary way to reduce noise or extract relevant information from specific aspects of the sensor output.

The vertical cilium is produced using a three-dimensional assembly technique called plastic deformation magnetic assembly (PDMA) [29]. The schematic of the process is shown in figure 2. To illustrate the principle we use a simple configuration, which consists of a cantilever beam with a piece of electroplated magnetic material attached to it. The structure can be realized by using surface micromachining techniques with one layer of sacrificial material at the bottom. The cantilever beam is released by using sacrificial etching. Subsequently, an external magnetic field is applied from underneath the substrate. The cantilever beam, together with the magnetic piece, will be bent out of plane under the applied magnetic field. The result of this process is that the cantilever will be plastically deformed if the amount of bending is above a certain threshold, resulting in permanent displacement (i.e. the bent form is retained even after the magnetic field is removed). The magnetic field is applied globally underneath the wafer so that many structures on a wafer are activated in parallel. The magnetic field can be provided by an electromagnetic field or a piece of permanent magnet.

The scanning electron micrograph of a finished device is shown in figure 3. Note that there are a number of differences between the artificial haircell and the biological counterpart. The biological hair has a circular cross-section, whereas this artificial haircell has a rectangular cross-section. These shape differences produce pertinent departures from functionalities

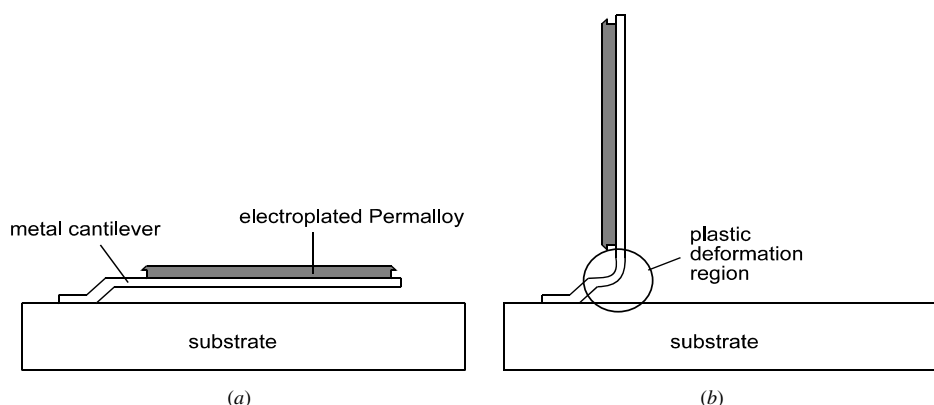


Figure 2. Schematic diagram of the PDMA process. (a) A representative cantilever with electroplated magnetic material attached and (b) magnetic actuation causes the cantilever beam to rotate off the substrate plane. Plastic deformation occurs near the anchor region.

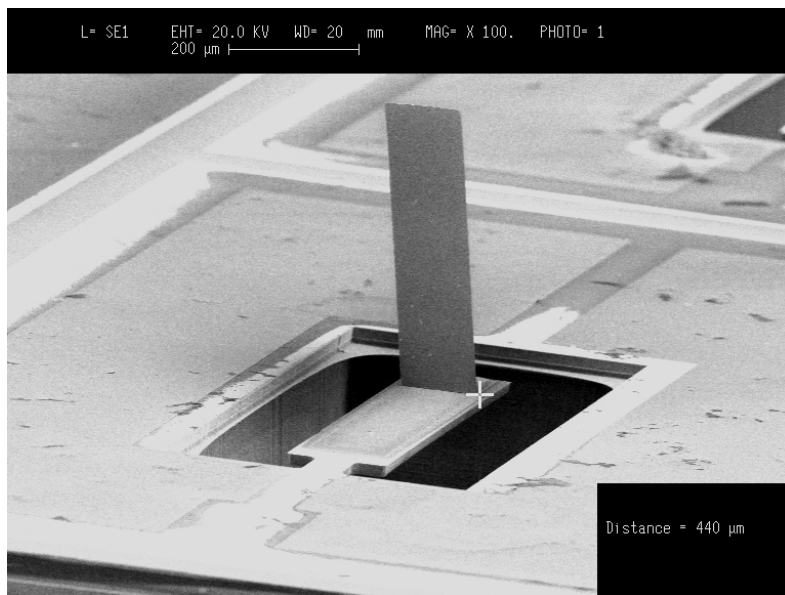


Figure 3. SEM of a single artificial haircell sensor. The cilium is $820\ \mu\text{m}$ tall. The strain gauge has a nominal resistance of $3\ \text{k}\Omega$. The strain gauge is $5\ \mu\text{m}$ wide and effectively $150\ \mu\text{m}$ long.

in biological systems for some sensing applications. For example, if the haircells are used for flow sensing, the asymmetrical cross-section will introduce different directional sensing behavior in response to an equal force on the broad versus narrow face. The artificial haircell is not as mechanically robust as the biological one, since the beam is made of single crystal silicon and the joint between the hair and the horizontal silicon beam is made of metal. These issues are addressed in the work on polymer-based haircell sensors discussed in the following section. Alternatively, the hair in this device can be made of other materials and processes, such as SU8 epoxy [26].

Basic fluid testing of the sensor has been conducted by mounting sensors on a thin glass plate, which is placed within a laminar flow water tunnel. One edge of the glass is polished to present a sharp profile facing the flow to reduce flow disturbances and introduce controlled boundary conditions. The sensor is located $1\ \text{mm}$ from the leading (sharp) edge. The flow rate of the water tunnel is varied manually to produce a laminar flow past the sensor element with u_0 ranging from 0 to $1\ \text{m s}^{-1}$ (figure 3). The flow impacts the cilium at its broad side, i.e. parallel to the long axis of the substrate cantilever. The sensor is biased under constant voltage ($1\ \text{V}$) and the output current is monitored. The output response is shown in figure 4, which illustrates that the best-fit curve follows a second-order polynomial expression, as expected from an earlier analysis.

Polymer-based artificial haircells

The schematic of a polymer-based artificial haircell sensor (AHC) is shown in figure 5. The AHC is composed of a vertical beam (artificial cilium) rigidly attached to the substrate. Attached at the base of the beam, between the cilium and the substrate, is a strain gauge. The strain gauge

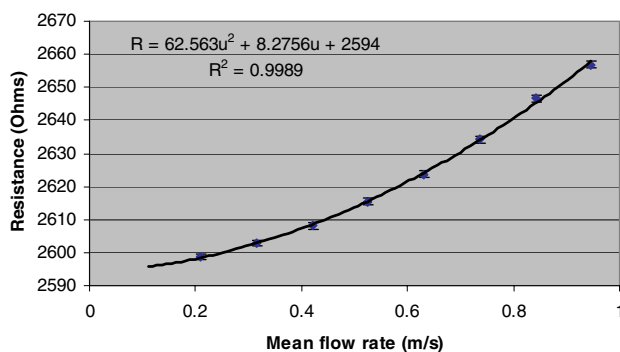


Figure 4. Measurement results showing output current versus flow rate of a representative sensor under constant voltage biasing.

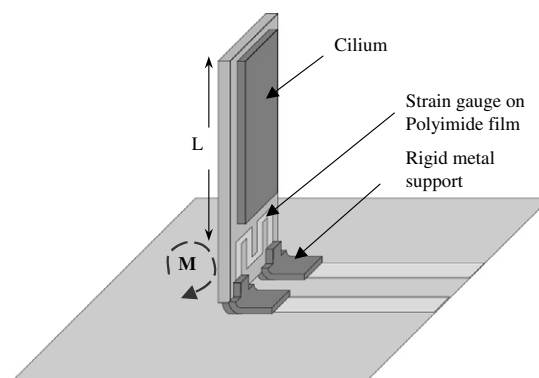


Figure 5. Schematic of an artificial haircell (protective top polyimide layer not drawn). The vertical part is surface micromachined and deflected out of plane using magnetic 3D assembly. The vertical portion will remain in a deflected position due to plastic deformation at the joint.

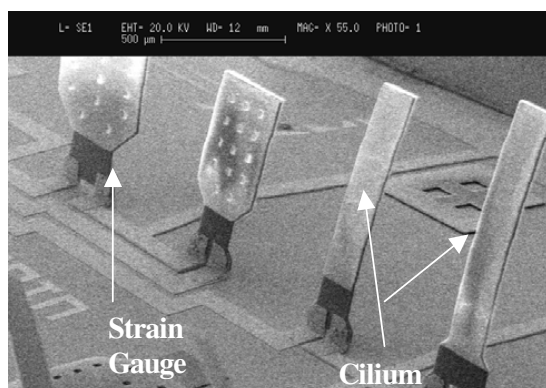


Figure 6. SEM of a fabricated haircell array with different heights and widths. The fabricated device has cilium length varying from $600\ \mu\text{m}$ to $1.5\ \text{mm}$. The strain gauge is not apparent because of the top protective polyimide coating.

comprises a thin film nichrome (NiCr) resistor on a thicker polyimide backing that runs the length of the cilium. The vertical hair is made by using the magnetic assembly process discussed in the previous section.

There are three major differences between this AHC and the silicon sensor discussed earlier. Specifically,

- (1) this AHC does not use a horizontal silicon beam;
- (2) this AHC used polyimide, a polymer material, as the haircell;
- (3) this AHC used metal as the strain gauge, instead of doped silicon.

As a result, this new device may have (1) a smaller overall footprint and (2) a more mechanically robust hair. The sensitivity of the metal strain gauge is generally ten times worse than that of the doped silicon piezoresistor in terms of sensing mechanical strain.

When an external force is applied to the vertical beam, either through direct contact with another object (functioning as a tactile sensor) or by the drag force from fluid flow (flow sensing), the beam will deflect and cause the strain gauge to stretch or compress. The strain gauge region is treated as being rigidly attached to the substrate, while the cilium is free. The magnitude of the induced strain (ε) is largest at the base, where the strain gauge is located, $\varepsilon = \frac{Mt_{pi}}{2EI}$, where M is the moment experienced at the base, t_{pi} the polyimide thickness and E and I are the modulus of elasticity and the moment of inertia of the polyimide respectively.

An array of AHC with different cilium and strain gauge geometry is shown in figure 6, illustrating the parallel nature of the magnetic assembly fabrication process. Overall, the fabrication method does not exceed a temperature of $350\ ^\circ\text{C}$, allowing it to be completed on a skin-like thin film polymer substrate. Silicon, glass and Kapton film have all been used as a substrate for this process [24]. The resistance of the various devices tested ranges from $1.2\ \text{k}\Omega$ to $3.2\ \text{k}\Omega$; TCR measurement of the as-deposited NiCr film has a value of $-25\ \text{ppm}\ ^\circ\text{C}^{-1}$, which is very small and should not contribute to anemometric effects during airflow testing.

The fabricated haircells were tested as airflow transducers in a wind tunnel. The wind tunnel measurement of three AHCs

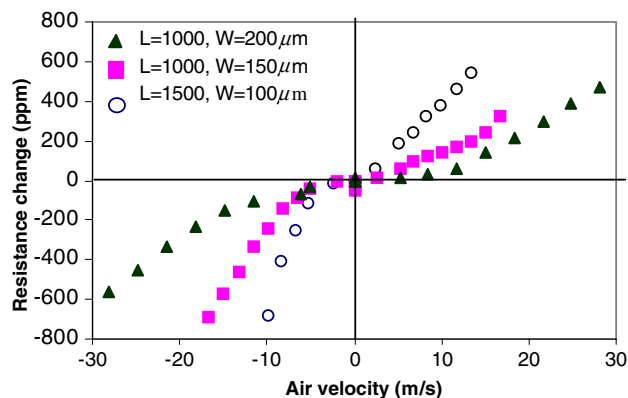


Figure 7. Airflow response of AHC inside a wind tunnel, using AHCs with various cilium widths and lengths. The velocity response can be tailored by changing the cilium geometry.

with different cilium geometry is plotted in figure 7. Two major conclusions can be drawn from this plot:

- (1) The response of each sensor is bidirectional—i.e. the sensor response changes signs depending on the direction of the applied flow.
- (2) The response sensitivity is a function of the area of the polyimide hair—the larger the paddle, the greater the flow-induced force under a given flow.

Additionally, the haircells can be made of even more robust polymer materials such as elastomers (including polydimethylsiloxane and polyurethane). A reference about the polyurethane-based artificial haircell sensor is discussed in [25, 30].

Yet another polymer-based haircell has been developed employing polyurethane (an elastomer) as the hair and carbon-nanotube-doped force-sensitive resistors as the sensing element. Polymers can be classified into three categories: fiber, plastics and elastomer. Whereas the polyimide material used in the previous work is a plastic, this new device uses elastomer that can undergo even larger deformation than plastics. This property increases the range of angular deformation and mechanical robustness.

The polymer AHC consists of a high aspect ratio polyurethane hair that is made using a modified lost-wax molding technique. It consists of a hair made of polyurethane. Four force-sensitivity resistors (FSRs) are located within the footprint of the polyurethane hair. These FSRs are arranged in four quadrants and a center-symmetric fashion in order to detect two-axis deflection of the cilium. Each of the four FSRs sits on top of a pair of interdigitated gold electrodes that allows measurement of the resistances of individual FSRs. Figure 8(a) illustrates the four FSRs and underlying electrodes before the hair is built on top of them. Transverse displacement of the hair tip causes normal stress to be applied to the FSR sensors; the stress could be compressive or tensile, depending on the direction of cilia displacement. The differential resistance changes from the four sensors provide an indication of both magnitude and direction of the force input.

Many biological sensors are preferentially sensitive to the directions of input signals in a single plane. They accomplish

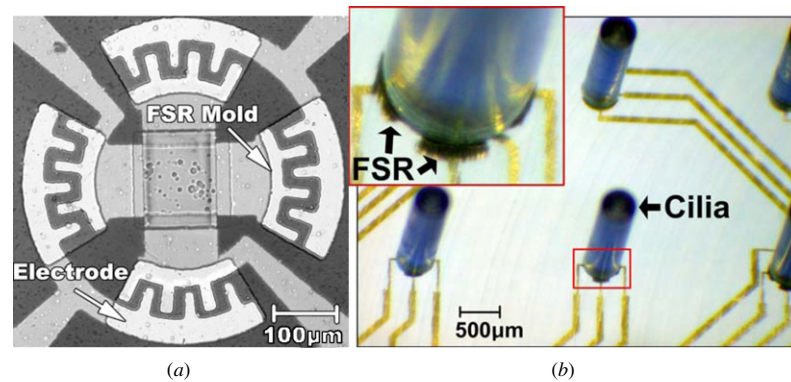


Figure 8. (a) Top view micrograph of interdigitated gold electrodes under four-quadrant FSRs. (b) Diagram showing relation of FSRs to the wiring and cilium structure.

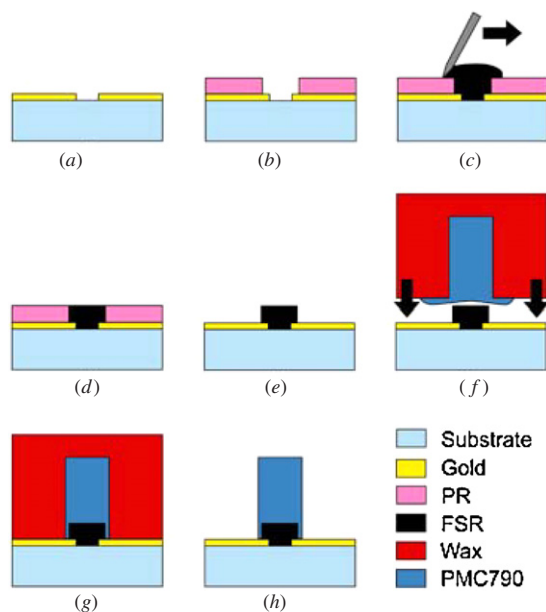


Figure 9. Fabrication flow: (a) deposition of gold wiring, (b) patterning of a photoresist mold, (c) filling mold with the FSR material and squeegee of excess the material, (d) curing of FSR, (e) removal of the PR mold, (f) alignment of urethane hair in a wax mold, (g) curing of urethane cilia and (h) removal of the wax mold.

the directionality through either a single sensor or a multi-sensory coupling. The engineering sensor discussed here is capable of directional sensing with a single sensor. One of the advantages is a small sensor footprint, which translates into small dimensions required of integrated circuit chips and lower costs. However, it should be noted that directional behavior of engineering sensors can be accomplished through the approach of multi-sensor coupling as well, which may provide certain advantages over the approach of relying on a single sensor. Such advantages may include a lower detection limit and better angular discrimination.

Fabrication starts by evaporating 2500 Å of gold onto the substrate (with a 50 Å thick chrome adhesion promoter layer). The backside alignment of the cilia mold requires an optically transparent substrate. Both glass and Kapton substrates satisfy this requirement and consequently have been used

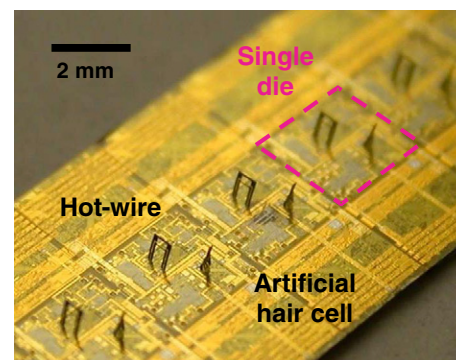


Figure 10. Photograph of the hot-wire array integrated with a constant-temperature feedback circuit. Artificial haircell sensors are also integrated on the same substrate, potentially allowing multi-modal, fully integrated flow sensors.

as substrates. Photoresist is spun and photolithographically patterned, and the gold layer is wet etched (figure 9(a)) to define wiring. Next, a 20 μm thick layer of AZ4620 photoresist is spun in two steps and patterned to define the molds for the FSRs (figure 9(b)). The two components of the carbon impregnated PMC121 polyurethane FSRs are then mixed manually with a blade, applied to the mold and degassed under vacuum. The excess FSR material is removed by squeegee action (figure 9(c)) [31]. The FSRs are allowed to cure overnight at room temperature (figure 9(d)). The photoresist mold for screen printing is removed (step (e)). Next, a small hole with dimensions of the hair is drilled in a piece of wax. The hole is filled with a polyurethane precursor and made to contact the silicon wafer at the registered location of the FSRs. The wax is then removed by dipping the device in hot water (step (h)).

Applications

The developed AHC sensors have been successfully tested as flow sensors as well as three-axis vibration sensors. The performance of the silicon-based AHC reaches a sensitivity of 0.5 mm s⁻¹ in water.

The AHC sensor has been assembled into linear arrays that are directly located on a silicon wafer with pre-existing signal processing circuitry as shown in figure 10. This constitutes an

artificial lateral line sensor and can be used in the future for underwater hydrodynamic imaging, vehicle maneuvering and threat detection/tracking. Together with suitable bioinspired signal processing algorithms [32], the artificial lateral line may provide underwater submersible vehicles with a new way of underwater detection, to complement sonar and vision.

Conclusions and discussions

Various generations of haircell sensors have been developed. A silicon-based AHC and two polymer-based AHC are discussed, illustrating their design, materials and performances in two cases. The silicon-based AHC provides the best sensitivity at this moment, whereas polymer-based sensors exhibit a high degree of robustness.

More research in the future will be aimed at developing haircells that are robust and yet highly sensitive, combining the high sensitivity of silicon material but taking advantage of advanced polymer materials.

The microfabrication process can be used to integrate other sensor modalities (that may not be haircell based) for data fusion. For example, we have demonstrated proof of concept of multimodal flow sensors, incorporating not only haircells but also sensors for measuring pressure and flow shear stress [33]. The multimodal sensing capability will further increase the ability of underwater imaging and control. For example, a sensor skin containing shear stress sensors and pressure sensors may generate more complete information about the flow field than the current generations of haircell sensor alone, provide for redundancy and calibration and extend the spatial range for flow sensing.

As the number of sensors increases, the signal conditioning becomes an important issue. There are several challenges: (1) signal processing generally requires semiconductor substrates, which do not provide mechanical deformability; (2) a large number of signals need to be processed local to the sensor to avoid noise associated with propagation leads; (3) the number of conductor leads must be reduced to avoid overcrowding the sensor chip with many nodes on them.

There are challenges in materials as well. Biological neurons and hairs are made of exquisite materials that offer functions and performance not available in engineering [34]. For example, biological materials, made of proteins, provide both robustness and stiffness at the same time. Engineering materials, on the other hand, can provide good robustness (e.g., elasticity) or large stiffness, but rarely at the same time. Using existing engineering materials often limits the performance of flow sensors and arrays. It is necessary to study the biological nanostructures, develop advanced materials and processing techniques and apply them in the microfabrication process to realize better sensors in the future.

It is the author's belief that research into biomimetic haircells will enrich biological understanding, initiate new engineering capabilities and enable new engineering functions. A large body of work remains to be explored. A direct comparison with biology using different animal species that vary in sensing requirements and tasks is important to establish

broad principles and to give insight into how to solve specific engineering design challenges. The current generations of biologically inspired haircells still do not compete with biological units in terms of their sensitivity, signal-to-noise ratio, sophistication and efficiency of signal processing, functional richness and dynamic range. More development work is underway to realize a flexible, low cost and multimodal sensing skin that incorporates signal processing electronics and robust/sensitive mechanical sensors.

Acknowledgments

The author wishes to thank the following funding agencies for cumulative support: NSF CAREER award, NASA, AFOSR (Bioinspired Concept program) and DARPA (Biological Sensory and Structure Emulation).

References

- [1] Delcomyn F 1996 *Foundations of Neurobiology* (New York: Freeman)
- [2] Dallos P and Evans B 1995 High-frequency motility of outer hair cells and the cochlear amplifier *Science* **267** 2006–9
- [3] Barth F G, Humphrey J A C and Secomb T W 2003 *Sensors and Sensing in Biology and Engineering* (Vienna: Springer)
- [4] Deocomyn F 1996 *Foundations of Neurobiology* (San Francisco: Freeman)
- [5] Bathellier B, Barth F G, Albert J T and Humphrey J A C 2005 Viscosity-mediated motion coupling between pairs of trichobothria on the leg of the spider *Cupiennius Salei* *J. Compar. Physiol. A* **191** 733–46
- [6] Barth F G, Humphrey J A C and Secomb T W 2003 *Sensors and Sensing in Biology and Engineering* (Vienna: Springer)
- [7] Engelmann J, Hanke W, Mogdans J and Bleckmann H 2000 Hydrodynamic stimuli and the fish lateral line *Nature* **408** 51–2
- [8] Liao J C, Beal D N, Lauder G V and Triantafyllou M S 2003 Fish exploiting vortices decrease muscle activity *Science* **302** 1566–9
- [9] Engelmann J, Hanke W and Bleckmann H 2002 Lateral line reception in still- and running water *J. Compar. Physiol. A* **188** 513–26
- [10] Miller G 2005 Bats have a feel for flight *Science* **310** 1260–1
- [11] Galvao R, Israeli E, Song A, Tian X, Bishop K, Swartz S and Breuer K 2006 The aerodynamics of compliant membrane wings modeled on mammalian flight mechanics presented at *36th AIAA Fluid Dynamics Conference and Exhibit* (San Francisco)
- [12] Singla V and Reiter J F 2006 The primary cilium as the cell's antenna: signaling at a sensory organelle *Science* **313** 629–33
- [13] He D Z Z and Dallos P 1999 Somatic stiffness of cochlear outer hair cells is voltage-dependent *Proc. Natl Acad. Sci.* **96** 8223–8
- [14] Liu C 2005 *Foundations of MEMS* (Englewood Cliffs, NJ: Prentice-Hall)
- [15] Ozaki M, Wada-Katsumata A, Fujikawa K, Iwasaki M, Yokohari F, Satoji Y, Nisimura T and Yamaoka R 2005 Ant nestmate and non-nestmate discrimination by a chemosensory sensillum *Science* **309** 311–4
- [16] Schaller R R 1997 Moore's law: past, present, and future *IEEE Spectr.* **34** 52–9
- [17] Ghosh S, Sood A K and Kumar N 2003 Carbon nanotube flow sensors *Science* **299** 1042–4
- [18] Svensson L, Plaza J A, Benitez M A, Esteve J and Lora-Tamayo E 1996 Surface micromachining technology

- applied to the fabrication of a FET pressure sensor
J. Micromech. Microeng. **6** 80–3
- [19] Wur D R, Davidson J L, Kang W P and Kinser D L 1995 Polycrystalline diamond pressure sensor
J. Microelectromech. Syst. **4** 34–41
- [20] Wang L, Wold R A, Wang Y, Deng K K, Zou L, Davis R J and Troler-McKinstry 2003 Design, fabrication, and measurement of high-sensitivity piezoelectric microelectromechanical systems accelerometers
J. Microelectromech. Syst. **12** 433–9
- [21] Bernstein J, Miller R, Kelley W and Ward P 1999 Low-noise MEMS vibration sensor for geophysical applications
J. Microelectromech. Syst. **8** 433–8
- [22] Madou M J 2002 *Fundamentals of Microfabrication: The Science of Miniaturization* 2nd edn (Boca Raton, FL: CRC Press)
- [23] Li J, Fan Z, Chen J, Zou J and Liu C 2002 High yield microfabrication process for biomimetic artificial haircell sensors, Presented at *Smart Electronics, MEMS, and Nanotechnology Conference, Proc. SPIE* **4700** 315–22
- [24] Chen J, Fan Z, Zou J, Engel J and Liu C 2003 Two dimensional micromachined flow sensor array for fluid mechanics studies *ASCE J. Aerospace Eng.* **16** 85–97
- [25] Engel J, Chen J, Bullen D and Liu C 2005 Polyurethane rubber as a MEMS material: characterization and demonstration of an all-polymer two-axis artificial haircell flow sensor, presented at *18th IEEE Int. Conf. Micro Electro Mechanical Systems, MEMS 2005 (Miami Beach, FL, 2005)*
- [26] Chen N, Chen J, Engel J, Pandya S, Tucker C and Liu C 2006 Development and characterization of high sensitivity bioinspired artificial haircell sensor, Presented at *The 12th Solid State Sensors, Actuator, and Microsystems Workshop (Hilton Head, SC, 2006)*
- [27] Krijnen G J M, Dijkstra M, van Baar J J, Shankar S S, Kuipers W J, de Boer R J H, Altpeter D, Lammerink T S J and Wiegerink R 2006 MEMS based hair flow-sensors as model systems for acoustic perception studies
Nanotechnology **17** S84–9
- [28] Ozaki Y, Ohyama T, Yasuda T and Shimoyama I 2000 An air flow sensor modeled on wind receptor hair of insects, Presented at *Int. Conf. MEMS (Miyazaki, Japan, 2000)*
- [29] Zou J, Chen J, Liu C and Schutt-Aine J 2001 Plastic deformation magnetic assembly (PDMA) of out-of-plane microstructures: technology and application *IEEE/ASME J. Microelectromech. Syst.* **10** 302–9
- [30] Engel J, Chen J, Liu C and Bullen D 2006 Polyurethane rubber all-polymer artificial hair cell sensor *IEEE/ASME J. Microelectromech. Syst.* **15** 729–36
- [31] Ryu K, Wang X, Shaikh K and Liu C 2004 A method for precision patterning of silicone elastomer and its applications *J. Microelectromech. Syst.* **13** 568–75
- [32] Pandya S D, Yang Y, Jones D, Engel J and Liu C 2006 Multisensor processing algorithms for underwater dipole localization and tracking using MEMS artificial lateral line sensors *EURASIP J. Appl. Signal Process.* **2006** art id 76593
- [33] Fan Z, Engel J M, Chen J and Liu C 2004 Parylene surface-micromachined membranes for sensor applications *J. Microelectromech. Syst.* **13** 484–90
- [34] Mayer G 2005 Rigid biological systems as models for synthetic composites *Science* **310** 1144–7